Computer Science and Information Technologies
Vol. 2, No. 2, July 2021, pp. 49~57
ISSN: 2722-3221, DOI: 10.11591/csit.v2i2.p49-57

Design and simulation of high-swing fully differential telescopic Op-Amp

Zahra Pezeshki
Faculty of Electrical and Robotic Engineering, Shahrood University of Technology, Shahrood, Semnan, Iran

Article Info

Article history:

Received Oct 1, 2020
Revised Feb 10, 2021
Accepted Feb 17, 2021

Keywords:

Output swing
Phase margin
Slow rate
Telescopic operating amplifier
Unity-gain frequency

ABSTRACT

This article describes the process of design and simulation of a high-swing fully differential telescopic operational amplifier (Op-Amp). Due to the common gate-common source (CG and CS) cascode structure, the gain is very high. To maximize this gain, the load must also be selected such as two current sources. This circuit has the higher voltage in output than current Op-Amps in accordance with desirable characteristics. The loss of power of this operating amplifier are very low and in milliwatts. With use of a power supply of 1.8 V, it achieves a high-swing 1.2 V, a differential gain of 76.333 dB, ω_{uGB} of 412 MHz, and >50 dB CMRR. This new design through the simulations and analytically shows that the high-swing fully differential telescopic Op-Amp retains its high CMRR even at high frequencies.

This is an open access article under the CC BY-SA license.

Corresponding Author:

Zahra Pezeshki
Faculty of Electrical and Robotic Engineering
Shahrood University of Technology
Shahrood, Semnan, Iran
Email: tejaratemrooz@gmail.com

1. INTRODUCTION

The simplest operational amplifier (Op-Amp) is a high-gain differential amplifier. The amount of this gain in the range of 10^1-10^5 is sufficient for Op-Amp applications. Op-Amp performance parameters are: open-loop gain, small signal bandwidth, large signal bandwidth, output swing, linearity, noise, offset and supply rejection [1], [2]. By designing an Op-Amp, these parameters are communicated with each other. Single cascode differential amplifiers with integrated components can hardly produce much gain. The bandwidth is determined by the load capacitance. To achieve the high gain, differential cascodes are used. These cascode connections lie between power supplies and load current sources. When the MOSFETs of each branch are aligned with each other, they create a telescopic-like structure. Therefore, this type of configuration is known as telescopic Op-Amp. The resulting circuit is symmetric with each of the output loads generated by the cascade current source. Their output swings are also limited due to the short-circuit problem of one of the inputs to the output in the applications such as source follower [3]. Another problem is power consumption. There are various designs that they have tried to reach high swing with low power consumption, but the power consumption value has not been reported [3]. In some papers, output swing is low or has not been reported too [4], [5]. The gain-boosted telescopic Op-amps can reach to high swing with low power consumption, but their design is classified into multiple design:

a. folded cascode Op-amp [6].
b. the main Op-amp and the boosting Op-amp [7], [8].
c. the main Op-amp and the multiplying digital-to-analog converter (MDAC) architecture [9].
d. the main Op-amp and the Miller compensation [10].

So, such a design implementation is very complicated. In this paper, author want to design a high-swing fully differential telescopic Op-Amp in 0.18 µm CMOS technology. All simulations of this circuit are performed in HSPICE RF software. Other softwares such as Cadence can also be used in this regard [2].

Figure 1 shows the fully differential telescopic Op-Amp. The fully differential designs include the first and secondly switched current mirrors and the output which can be a circuit duo to boosting the gain and reaching the wide band [11]-[17], but this can cause the power consumption to increase. Biasing also can improve the gain with less dissipation, e.g. wideband QFG dynamic biasing (QFG-DB) Op-amp, but it cannot to increase the output or input voltage [18]. Some applications such as fully differential difference transconductance amplifier (FDDTA), require low output, so the high gain is not important in their design. Because they are utilized as a low pass filter [19]. The advantage of the fully differential design is that the differential mode signal path encompasses only the n-channel MOSFETs [20]. Only NMOS transistors conduct time-varying currents, and PMOS transistors transmit a constant current. This increases the Op-Amp speed, so the mobility of the n-channel MOSFET is greater than that of the p-channel MOSFET. In my design, we use the telescopic Op-Amp [8] of Figure 1. It is a combination of common gate-common source (CS-CG) that achieves higher gain due to double load of current source.

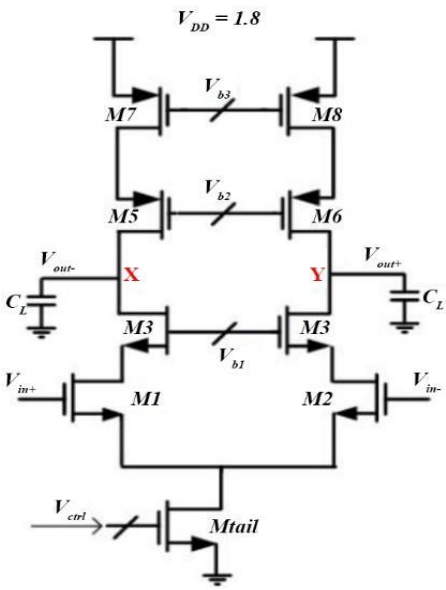

Figure 1. Telescopic cascode with NMOS inputs

Combination of CS-CG cascodes with components such as NMOS is for higher gain. Cascade load current sources with components such as PMOS are used to achieve greater drain resistance, which is used to combine CS-CG cascodes. The gain of the circuit in Figure 1 can be obtained by using half of the circuit as (1) [21].

$$A = g_{mN}[(g_{mN}r_{ON}^2) \parallel (g_{mP}r_{OP}^2)] \quad (1)$$

Where g_m is the cross-conductivity and r_O is the drain resistors in the MOSFETs. So, the gain of the telescopic cascode Op-Amp increases. The output swing is as (2):

$$V_{cmo} = 2[V_{DD} - (V_{OD1} + V_{OD3} + V_{ODtail} + |V_{OD5}| + |V_{OD7}|] \quad (2)$$

Where, the V_{OD} is overdrive voltage of the MOSFETs, and V_{ODtail} reduce through the Mtail MOSFET current source, I_{total}. The output voltage of this circuit is much less than that of a simple fully differential Op-Amp. So, in this paper, I want to design a new fully differential telescopic Op-amp with specifications as shown in Table 1.

Table 1. The characteristic of high-swing fully differential telescopic OP-AMP circuit

Parameter	Characteristic
Gain	> 60 dB
CMRR	> 50 dB
ω_{uGB}	> 2π × 400 MHz
Phase margin	> 60
Slow Rate	> 200 V/μs
V_{cmi}	= 1 V
V_{cmo}	= 1.1 V
Output Swing	> 0.5 V
Power Consumption	> = 1.2 mW
Power supply (V_{DD})	1.8 V

2. THE PROPOSED METHOD

According to the Table 1, author must also consider other features of the telescopic cascade and add to the MOSFETs including $\mu_n C_{ox} = 200\frac{\mu A}{V^2}$, $\mu_p C_{ox} = 80\frac{\mu A}{V^2}$, body modulation effects: $\lambda_n = 0.18\,V^{-1}$ and $\lambda_p = 0.36\,V^{-1}$, and the threshold voltage: $V_{THN} = |V_{THP}| = 0.45\,V$ [3], [4]. In this circuit, the total power consumption should not exceed 1.2 mW. The current source of V_{DD} is $I_{tail} = 1.2\frac{mW}{1.80}$ $V = 0.67\,mA$. So, each cascode branch of the Op-Amp requires 0.34 mA current, means $I_{tail}/2$. On the other hand, the common mode output voltage is 1.1 V. That is, each node X and Y in Figure 1 should be able to swing up to 1.1 volt and keep the transistors $M_3 - M_6$ in saturation area. With a 1.8 V power supply, the total voltage available for M_{tail} and each cascode branch is 0.7 V. Thus, we have (3):

$$V_{OD1} + V_{OD3} + |V_{OD5}| + |V_{OD7}| + V_{ODtail}] = 1.8 - 1.1 = 0.7 \tag{3}$$

Since M_{tail} draws most of the current, one fifth of the voltage reaches to it, so $V_{ODtail} = 0.14\,V$ and $0.56\,V$ remains for the four cascade transistors. The $M_5 - M_8$ current sources have low mobility, so more voltage should be allocated per branch to them ($0.32\,V$). Therefore, in a cascade branch, we have $V_{OD5} + V_{OD7} = 0.32\,V$. The rest of the voltage is allocated to transistors M_1 and M_3. That is $V_{OD1} + V_{OD3} = 0.24\,V$. So, the overdrive voltage of transistors 5 and 7 is $0.16\,V$ and the voltage of transistors 1 and 3 is $0.12\,V$. The aspect ratio of $M_1 - M_{tail}$ can be evaluated by the bias current and the overdrive voltage of each MOSFET. The relation of drain current to saturation area is (4):

$$I_D = (1/2)\mu C_{ox}(W/L)(V_{GS} - V_{TH})^2 \tag{4}$$

To minimize the parasitic capacitors of the integrated devices, the minimum length of each MOSFET transistor is $L = 0.18\,\mu m$.

Then, $(W)_{1-4} = 38\,\mu m$, $(W)_{5-8} = 58.25\,\mu m$ and $W_{tail} = 58.775\,\mu m$ are obtained. So, the design was done according to the total power consumption, power supply and output swing. The amount of the gain can now be calculated from the (5),

$$A_v \approx g_{m1}[(g_{m3}r_{o3}r_{o1}) \parallel (g_{m5}r_{o5}r_{o7})] \tag{5}$$

By choosing a minimum channel length of $0.18\,\mu m$ for all MOSFET transistors we have g_m and r_o which are obtained from (6) and (7).

$$g_m = 2I_D/V_{OD} \tag{6}$$

$$r_o = 1/\lambda I_D \tag{7}$$

So, author have:

$$g_{m1-4} = \frac{2 \times 0.32 \times 10^{-3}}{0.123} = 5.203\frac{mA}{V}$$

$$g_{m5-8} = \frac{2 \times 0.32 \times 10^{-3}}{0.157} = 4.764\frac{mA}{V}$$

$$r_{o1-4} = \frac{1}{0.18 \times 0.32 \times 10^{-3}} \approx 17361.11\ \Omega$$

$$r_{o5-8} = \frac{1}{0.36 \times 0.32 \times 10^{-3}} \approx 8680.56\ \Omega$$

In this paper, author propose the circuit of Figure 2, called high-swing fully differential telescopic Op-Amp.

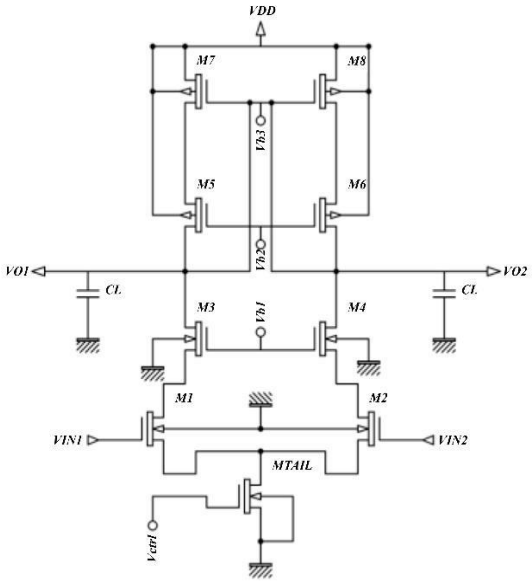

Figure 2. The proposed high-swing fully differential telescopic Op-Amp circuit

For doing simulation, firstly author must get the working point of all transistors using the “op" command (all transistors are in saturation area) see Figure 3.

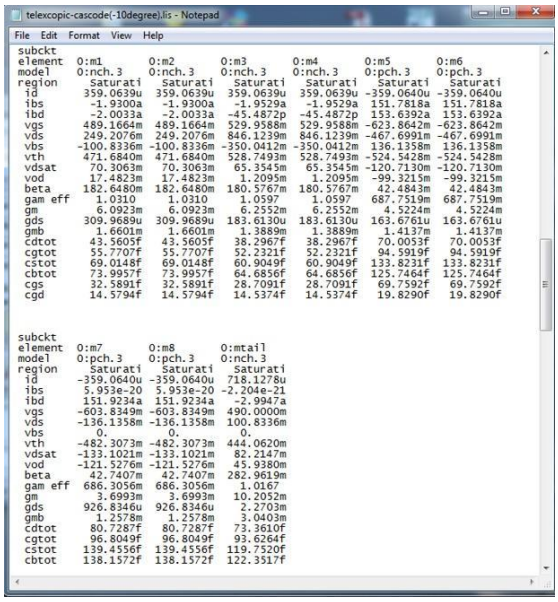

```
subckt
element  O:m1        O:m2        O:m3        O:m4        O:m5        O:m6
model    O:nch.3     O:nch.3     O:nch.3     O:nch.3     O:pch.3     O:pch.3
region     Saturati    Saturati    Saturati    Saturati    Saturati    Saturati
 id       359.0639u   359.0639u   359.0639u   359.0639u  -359.0640u  -359.0640u
 ibs       -1.9300a    -1.9300a    -1.9529a    -1.9529a   151.7818a   151.7818a
 ibd       -2.0033a    -2.0033a   -45.4872p   -45.4872p   153.6392a   153.6392a
 vgs      489.1664m   489.1664m   529.9588m   529.9588m  -623.8642m  -623.8642m
 vds      249.2076m   249.2076m   846.1239m   846.1239m  -467.6991m  -467.6991m
 vbs     -100.8336m  -100.8336m  -350.0412m  -350.0412m   136.1358m   136.1358m
 vth      471.6840m   471.6840m   528.7493m   528.7493m  -524.5428m  -524.5428m
 vdsat     70.3063m    70.3063m    65.3545m    65.3545m  -120.7130m  -120.7130m
 vod       17.4823m    17.4823m     1.2095m     1.2095m   -99.3215m   -99.3215m
 beta     182.6480m   182.6480m   180.5767m   180.5767m    42.4843m    42.4843m
 gam eff    1.0310      1.0310      1.0597      1.0597    687.7519m   687.7519m
 gm         6.0923m     6.0923m     6.2552m     6.2552m     4.5224m     4.5224m
 gds      309.9689u   309.9689u   183.6130u   183.6130u   163.6761u   163.6761u
 gmb        1.6601m     1.6601m     1.3889m     1.3889m     1.4137m     1.4137m
 cdtot     43.5605f    43.5605f    38.2967f    38.2967f    70.0053f    70.0053f
 cgtot     55.7707f    55.7707f    52.2321f    52.2321f    94.5919f    94.5919f
 cstot     69.0148f    69.0148f    60.9049f    60.9049f   133.8231f   133.8231f
 cbtot     73.9957f    73.9957f    64.6856f    64.6856f   125.7464f   125.7464f
 cgs       32.5891f    32.5891f    28.7091f    28.7091f    69.7592f    69.7592f
 cgd       14.5794f    14.5794f    14.5374f    14.5374f    19.8290f    19.8290f


subckt
element  O:m7        O:m8        O:mtail
model    O:pch.3     O:pch.3     O:nch.3
region     Saturati    Saturati    Saturati
 id      -359.0640u  -359.0640u   718.1278u
 ibs       5.953e-20   5.953e-20  -2.204e-21
 ibd      151.9234a   151.9234a   -2.9947a
 vgs     -603.8349m  -603.8349m   490.0000m
 vds     -136.1358m  -136.1358m   100.8336m
 vbs        0.          0.          0.
 vth     -482.3073m  -482.3073m   444.0620m
 vdsat   -133.1021m  -133.1021m    82.2147m
 vod     -121.5276m  -121.5276m    45.9380m
 beta      42.7407m    42.7407m   282.9619m
 gam eff  686.3056m   686.3056m     1.0167
 gm         3.6993m     3.6993m    10.2052m
 gds      926.8346u   926.8346u     2.2703m
 gmb        1.2578m     1.2578m     3.0403m
 cdtot     80.7287f    80.7287f    73.3610f
 cgtot     96.8049f    96.8049f    93.6264f
 cstot    139.4556f   139.4556f   119.7520f
 cbtot    138.1572f   138.1572f   122.3517f
```

Figure 3. Working point of the proposed high-swing fully differential telescopic Op-Amp circuit

To keep the all transistors in the saturation area, the bias voltages, control voltage, and maximum and minimum input voltages, V_{CMI}, are calculated to drive the transistors to the saturation area as:

$$V_{ctrl} = V_{GStail}\ if\ V_{ODtail} > V_{GStail} - V_{th}$$
$$V_{b1} = V_{GS3} + V_{ODM1} + V_{ODtail}\ if\ V_{OD3} > V_{GS3} - V_{th}$$
$$V_{b2} = V_{DD} - V_{ODM7} - V_{GS5}\ if\ V_{OD5} < V_{GS5} - V_{th}$$
$$V_{b3} = V_{DD} - V_{GS7}\ if\ V_{OD7} < V_{GS7} - V_{th}$$
$$\{V_{inMax} = V_{DD} - 2V_{OD7} - V_{OD3}\ and\ V_{inmin} = V_{GS1} + V_{ODtail}\ if\ V_{OD1} > V_{Gs1} - V_{th}\}$$

So after simulation, all transistors are active and their current are regulated which the total power consumption of the circuit obtains as 1.2 mW see Figure 4.

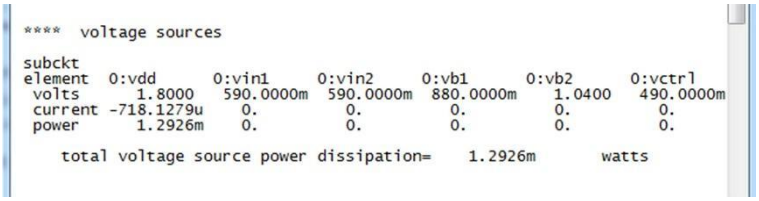

```
****  voltage sources

subckt
element  0:vdd      0:vin1     0:vin2     0:vb1      0:vb2      0:vctrl
 volts      1.8000   590.0000m  590.0000m  880.0000m   1.0400   490.0000m
 current -718.1279u    0.         0.         0.         0.         0.
 power      1.2926m    0.         0.         0.         0.         0.

    total voltage source power dissipation=    1.2926m       watts
```

Figure 4. Power consumption of the circuit (P_{diss}).

3. RESULTS AND DISSCUSION

In this section, author want to discuss about the simulation. According to the Figure 4, the current drawn from the power supply is 0.72 mA and the total power consumption of the circuit is 1.2 mW. The output voltage response as shown in Figure 5 is 1.2 V.

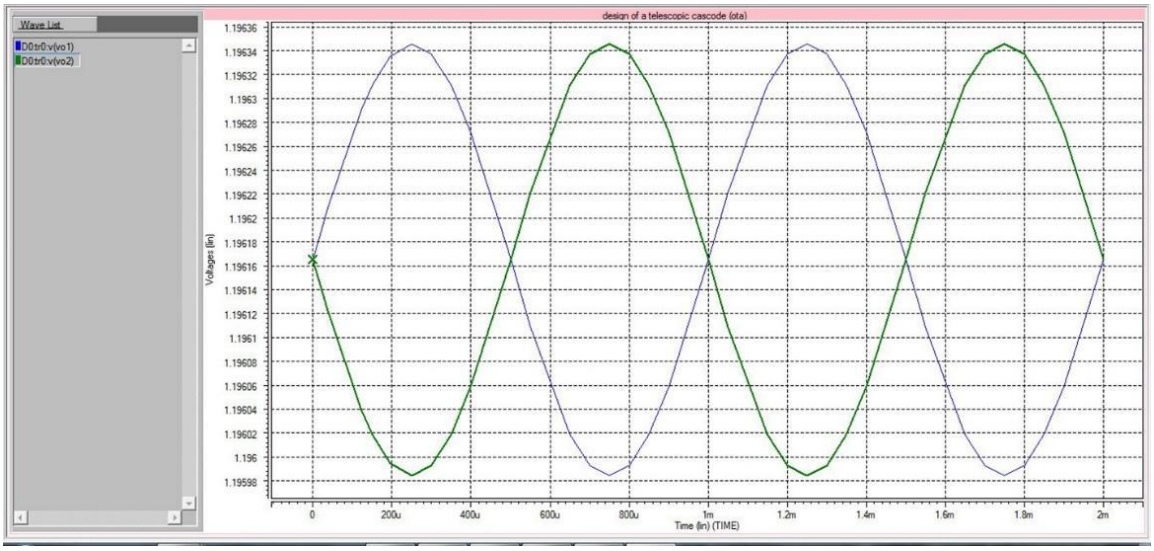

Figure 5. The output swing of the proposed high-swing fully differential telescopic Op-Amp circuit

In Figure 6, the circuit gain is greater than 60 dB and 76.333 dB ($111.75 - 35.417 = 76.333\ dB$). So, the Common Mode Rejection Ratio (CMRR) is greater than 50 dB.

At frequency of 412 MHz, the gain reaches one and thus the unity-gain frequency value, ω_{UGB}, is 412 MHz see Figure 7.

According to the Figure 7, at the $\omega_{UGB} = 412\ MHz$, the output phase value of the system is $-61.7°$, so the phase margin (PM) of the circuit is $180℃ - 61.7℃ = 118.3℃$, which a desirable value is. Further, the total harmonic distortion (THD) of the circuit is 0.332% for both V_{O1} and V_{O2} outputs see Figure 8.

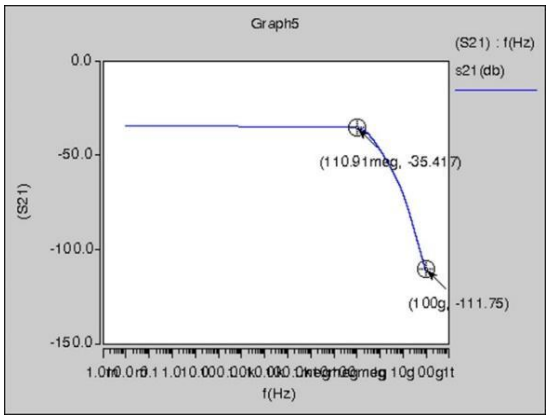

Figure 6. Frequency response of the proposed high-swing fully differential telescopic Op-Amp circuit

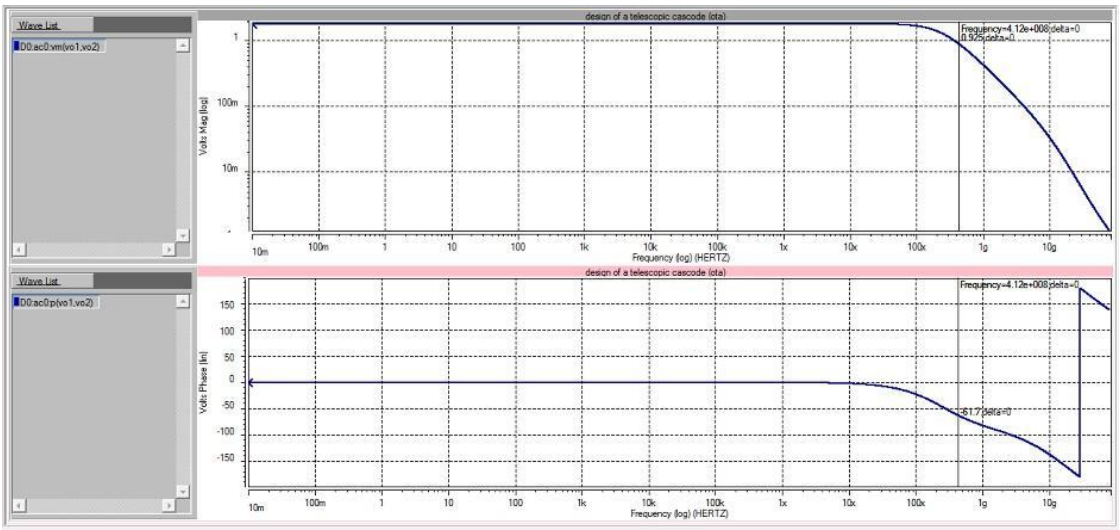

Figure 7. The ω_{UGB} and the output system phase of the proposed high-swing fully differential telescopic Op-Amp circuit

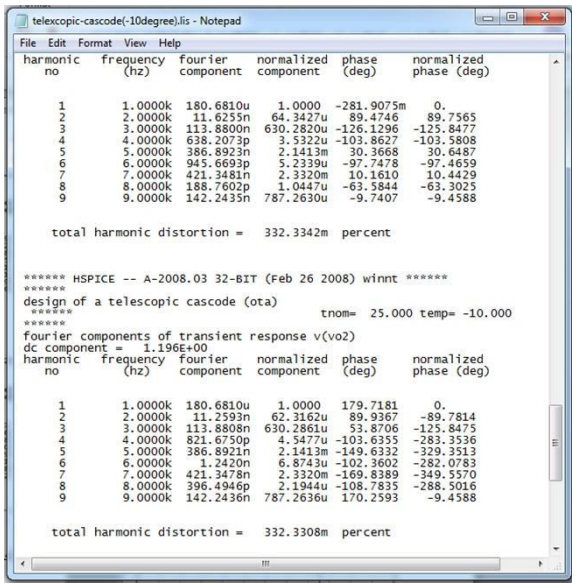

```
telexcopic-cascode(-10degree).lis - Notepad
File  Edit  Format  View  Help
 harmonic   frequency  fourier    normalized  phase     normalized
    no        (hz)     component  component   (deg)     phase (deg)

      1       1.0000k  180.6810u    1.0000  -281.9075m    0.
      2       2.0000k   11.6255n   64.3427u   89.4746    89.7565
      3       3.0000k  113.8800n  630.2820u -126.1296  -125.8477
      4       4.0000k  638.2073p    3.5322u -103.8627  -103.5808
      5       5.0000k  386.8923n    2.1413m   30.3668    30.6487
      6       6.0000k  945.6693p    5.2339u  -97.7478   -97.4659
      7       7.0000k  421.3481n    2.3320m   10.1610    10.4429
      8       8.0000k  188.7602p    1.0447u  -63.5844   -63.3025
      9       9.0000k  142.2435n  787.2630u   -9.7407    -9.4588

    total harmonic distortion =   332.3342m  percent


****** HSPICE -- A-2008.03 32-BIT (Feb 26 2008) winnt ******
******
design of a telescopic cascode (ota)
 ******                                  tnom=  25.000 temp= -10.000
******
fourier components of transient response v(vo2)
dc component =   1.196E+00
harmonic   frequency  fourier    normalized  phase     normalized
    no        (hz)     component  component   (deg)     phase (deg)

      1       1.0000k  180.6810u    1.0000   179.7181     0.
      2       2.0000k   11.2593n   62.3162u   89.9367   -89.7814
      3       3.0000k  113.8808n  630.2861u   53.8706  -125.8475
      4       4.0000k  821.6750p    4.5477u -103.6355  -283.3536
      5       5.0000k  386.8921n    2.1413m -149.6332  -329.3513
      6       6.0000k    1.2420n    6.8743u -102.3602  -282.0783
      7       7.0000k  421.3478n    2.3320m -169.8389  -349.5570
      8       8.0000k  396.4946p    2.1944u -108.7835  -288.5016
      9       9.0000k  142.2436n  787.2636u  170.2593    -9.4588

    total harmonic distortion =   332.3308m  percent
```

Figure 8. The THD of the proposed high-swing fully differential telescopic Op-Amp circuit

Author can calculate the slow rate as (8) [7], [22].

$$SR \equiv dV_{OUt}/dt|_{Max} = I_{tail}/C_L = (2I_{DM1.2})/C_L \quad (8)$$

Where $I_{DM1.2}$ is the bias current of transistors 1 and 2. The value of the slow rate is obtained 261.25 volts per microsecond (MHz) from the simulation see Figure 9.

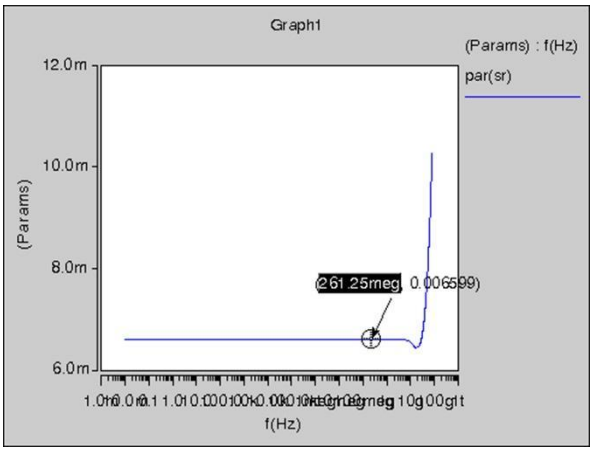

Figure 9. The slow rate of high-swing fully differential telescopic Op-Amp circuit

For noise analysis, I have to send the noise to the system, for example, with a 50 ohmic pull-up resistor (p1): p1 in 0 port=1 ac=0.1 dc=2.1 z0=50

The resistance value from the V_{O1} output to V_{DD} is calculated $g_{m5}r_{o5}r_{o7}$, which is 359 $k\Omega$. The output noise is 101.9337$\mu Volts$ see Figure 10.

```
**** the results of the sqrt of integral (v**2 / freq)
     from fstart upto   71.6382g      hz. using more freq points
     results in more accurate total noise values.

**** total output noise voltage   =  101.9337u       volts
**** total equivalent input noise =    0.
```

Figure 10. The output noise of the proposed high-swing fully differential telescopic Op-Amp circuit

The characteristic table of the proposed high-swing fully differential telescopic Op-Amp circuit is as Table 2.

Table 2. The Characteristic of the proposed high-swing fully differential telescopic OP-Amp circuit

Characteristic	Description
Power supply	1.8V
Power consumption	1.2 mW
Gain	76.333 dB
ω_{UGB}	412 MHz
Output Phase Value	-61.7°
PM	118.3°
THD	0.332%
Slow Rate	261.25 MHz
Total Output Noise Voltage	101.9337 µV
Output Swing Voltage	1.2 V
CMRR	> 50dB

The value of $(A_v \times \omega_{UGB})/P_{diss}$ obtains as:

$$(A_v \times \omega_{UGB})/P_{diss} = (76.333 \times 412 \times 10^6)/(1.2 \times 10^{-3}) \cong 26207.7 \times 10^9 dB \cdot Hz/Watt$$

The characteristic of this proposed Op-amp is good comparing the other Op-amps. Table 3 compares the characteristic of this Op-amp with other designs.

Table 3. Comparison the Characteristic of the proposed high-swing fully differential telescopic OP-Amp circuit with other circuits

Characteristic	The proposed Op-amp	QFGDB op-amp [3]	Fully Differential Gain-Boosted Telescopic Cascode Op-amp [7]	Telescopic Op-amp for MDAC [9]	High-Swing CMOS Telescopic Operational Amplifier [8]	Folded-cascode Op-amp [6]	Telescopic Op-Amp with Improved Gain [10]	Dc-Gain Enhanced CMOS Telescopic Op-Amp [5]	Fully-differential Op-amp [15]
Power supply	1.8	< 1	3.3	1.8	3.3	3.3	5	-	1.8
Power consumption (mW)	1.2	-	3.89	0.051	-	9-14	-	5	-
Gain (dB)	76.333	60.5	129	62.81	105	-	85	> 61	> 60
ω_{UGB} (MHz)	412	65	161	285.6	93	1.3GHz	177.1	1GHz	> 50
Output Phase Value (°)	-61.7	-	-	-	-	-	-	-	-
PM (°)	118.3	81	70.6	57.42	78	-	-	81	60
THD (%)	0.332	-	-	-	-	-	-	-	-
Slow Rate (V/µs)	261.25	-	92	2.19	133	-	-	-	> 100
Total Output Noise Voltage (µV)	101.9337	-	-	-	-	-	-	-	-
Output Swing Voltage (V)	1.2	-	3	-	2.4	-	-	-	> 2.7
CMRR (dB)	>50	>50	>50	-	>50	-	-	-	-

4. CONCLUSION

This paper presents the design of an of high-swing fully differential telescopic Op-Amp circuit with 0.18 CMOS technology. The results of the circuit simulation with HSPICE RF software show that the circuit parameters have acceptable values. One of the important features that this paper wants to acquire is higher voltage than current Op-Amps in accordance with desirable parameters. Finally, by compromising the circuit parameters, we were able to obtain a good performance from the circuit design. As the amplification of signals in many electronic circuits plays a key role and can be easily implemented with Op-Amp, this design can demonstrate this reality which can implemented in a Very Large-Scale Integration (VLSI) chip.

ACKNOWLEDGEMENTS

This paper is a technical report related to the Linear IC course which has been performed in Shahrood University of Technology, Semnan, Iran.

REFERENCES

[1] A. Worapishet, A. Demosthenous and X. Liu, "A CMOS Instrumentation Amplifier With 90-dB CMRR at 2-MHz Using Capacitive Neutralization: Analysis, Design Considerations, and Implementation," in *IEEE Transactions on Circuits and Systems I: Regular Papers*, vol. 58, no. 4, pp. 699-710, April 2011, doi: 10.1109/TCSI.2010.2078850.

[2] H. Qiao, "Design of a CMOS Two-stage Fully Differential Operation Amplifier," *J. Phys.: Conf. Ser.* vol. 1449, no. 2020, pp. 012084, 2020.

[3] J. Ramirez-Angulo, M. Sawant, A. Lopez-Martin, and R.G. Carvajal, “A power efficient and simple scheme for dynamically biasing cascode amplifiers and telescopic op-amps,” *Integration, the VLSI journal*, vol. 41, no. 4, pp. 539–543, 2008.
[4] D.S. Shylu1, D. Jackuline Moni, and N. Brigit Francis, “Design and Analysis of Low Power Pseudo Differential Class-Ab Telescopic Operational Amplifier,” *International Journal of Research in Engineering and Technology*, vol. 3, no. 19, pp. 234-238, 2014, doi:10.15623/IJRET.2014.0319044.
[5] B. Alizadeh, Sadegh Mohammadzadeh Bazarchi, and A. Dadashi, “Dc-gain enhanced CMOS Telescopic op-amp, “*2011 Faible Tension Faible Consommation (FTFC)*,” Marrakech, pp. 91-94, 2011.
[6] A. Baradaran Rezaeii, K. Dadashi, and S. Mahdavi, “Gain-Bandwidth Enhancement in Folded-Cascode Op-Amp, “*2016 1st International Conference on New Research Achievements in Electrical and Computer Engineering*,” 2016. [Online] https://www.civilica.com/Paper-CBCONF01-CBCONF01_0070.html.
[7] Wang Jin and Qiu Yulin, "Analysis and design of fully differential gain-boosted telescopic cascode Op-Amp, “*Proceedings. 7th International Conference on Solid-State and Integrated Circuits Technology*,” Beijing, China, vol. 2, pp. 1457-1460, 2004, doi: 10.1109/ICSICT.2004.1436874.
[8] K. Gulati and Hae-Seung Lee, "A high-swing CMOS telescopic operational amplifier," in *IEEE Journal of Solid-State Circuits*, vol. 33, no. 12, pp. 2010-2019, Dec. 1998, doi: 10.1109/4.735542.
[9] A. Dendouga and S. Oussalah, “Telescopic Op-Amp Optimization for MDAC Circuit Design,” *Electronics*, vol. 20, no. 2, pp. 55-61, 2016.
[10] M. Suthar, N. Gupta, and P. Soni, “Proposed Telescopic Op-Amp with Improved Gain,” *International Journal of Scientific and Research Publications*, vol. 2, no. 2, pp. 1-3, 2012.
[11] G.L. Schaffer and C.A. Cupertino, “Fully differential autozeroing amplifier,” *United States Patent*, US 8.487.697 B2, 2013.
[12] S. Chakraborty, “Fully Differential Wideband Amplifier,” *NM6007 Analog IC Laboratory Course, NTU-MSc in Integrated Circuit Design*, Technische Univeritat Munchen, Nanyang Technological University, Technical report, 2017, doi: 10.13140/RG.2.2.28346.08645.
[13] N. Hossein-Zadeh, M. Daliri, S. Magierowski and E. Ghafar-Zadeh, "A Novel Fully Differential NMR Transciever," 2018 *IEEE Life Sciences Conference (LSC), Montreal*, QC, pp. 13-16, 2018, doi: 10.1109/LSC.2018.8572220.
[14] J. Huijsing, “Fully Differential Operational Amplifiers,” In: *Operational Amplifiers*. Springer, Cham, pp. 289-306, 2017, doi: 10.1007/978-3-319-28127-8_8.
[15] E. Balti, “Fully-differential opamp design,” University of Idaho, Department of Electrical and Computer Engineering, *Technical Report*, ECE-515 Analog Integrated Circuit Design, Sep 2018.
[16] R.J. Baker, “Fully-Differential Amplifier,” *United States Patent*, US 5.953.276, 1999.
[17] A. Fant, L.Sant, and P. Vernei Torta, “Input Common Mode Circuit for A Fully Differental Amplifer,” *United States Patent*, US 8.633,765 B2, 2014.
[18] J. Ramirez-Angulo, M. S. Sawant, R. G. Carvajal and A. J. Lopez-Martin, "New compact and power efficient dynamically biased cascode mirrors and telescopic op-amps," 2006 *IEEE International Symposium on Circuits and Systems*, Island of Kos, 2006, pp.2833-2836, doi: 10.1109/ISCAS.2006.1693214.
[19] F. Khateb, M. Kumngern, T. Kulej, and V. Kledrowetz, “Low-voltage fully differential difference transconductance amplifier,” *IET Circuits Devices Syst.*, vol. 12, no. 1, pp. 73-81, 2018.
[20] A.S. Sedra, and K.C. Smith, Microelectronic circuits theory and applications, Oxford University press, 7th edition, pp. 848-857, 2010.
[21] B. Razavi, *Design of analog CMOS Integrated Circuits*, Tata Megraw Hill, 2002 edition, pp. 291-307.
[22] T.C. Carusone D. Johns and K. Martin, *Analog Integrated Circuit Design*, Wiley, 2nd Ed., 2011, pp. 1-816.

BIOGRAPHIES OF AUTHOR

Zahra Pezeshki is a Master holder in Electronic Integrated Circuits. She’s worked on electronic circuit design and project management from 2002 to now as well as obtained one patent in 2007 for solving irrigation problems. Furthermore, she has cooperated with Iran Construction Engineering Organization (IRCEO) as a researcher since 2012 whereas she works on developing new BIM standards for construction industry. Currently, she works as an engineer, senior lecturer and a journalist working with IRCEO and Iranian press. She is greatly interested in energy issues, sustainability and optimization. Her research activities are highly in design, modeling, programming and manufacturing of electrical maps, electrical boards and AI devices to increase thermal comfort and save energy.